[Frontiers in Bioscience 2, f4-12, April 1, 1997]

MR IMAGING ANALYSIS OF HETEROGENEOUS LEIOMYOMAS OF THE UTERUS

Hyun Kwon Ha[3], Mi Kyung Jee[1], Hong Jae Lee, Bo Young Choe, Jong Sub Park[2], Jun Mo Lee[2], Sung Eun Nam-Koong[2]

Departments of Radiology, [1]Clinical Pathology, and [2]Obstet and Gynecol, Catholic University Medical College, Seoul, 137-701, Korea

TABLE OF CONTENTS

1. ABSTRACT

Thirty-six leiomyomas from the same number of patients that were heterogeneous on MR imaging were evaluated for analyzing their MR patterns and for differentiating each type of secondary changes by means of MR imaging-pathologic correlation. The tumors with a mean diameter of 9 cm could be classified into 4 patterns depending on the morphological appearance of signal intensity: speckled (n = 14); nodular (n = 11); cystic (n = 9); or indeterminate (n = 2). Speckled pattern was associated with a mild degree of hyaline or myxoid degeneration or focal necrosis. Nodular pattern was caused by necrosis or cellular leiomyoma, and cystic pattern was related to severe hyaline or myxoid degeneration or necrosis. Each type of secondary changes within leiomyomas showed distinctive MR findings, if they were severely involved. However, use of an additional contrast-enhanced study was necessary in some instances for further clarification. MR imaging has a potential in distinguishing each type of secondary changes that occur in leiomyomas.

Various degenerative changes occur in approximately 65 % of uterine leiomyomas, and are caused mainly by alteration in the blood supply originating from rapid growth, pregnancy, mechanical accident, and postmenopausal atrophy (8). These changes include hyaline, mucoid, or myxoid degeneration, calcification, cystic changes, necrosis (red degeneration), and fatty metamorphosis (2, 8, 12). It is well known that the presence of degenerative changes within leiomyomas can be predicted on MR imaging by a heterogeneous signal intensity on T2-weighted images (6), although clear distinction of each type of degeneration can not be made by this modality (1, 4, 14). Recently, cellular leiomyoma, one of the variants of leiomyomas, was also reported to cause heterogeneous signal intensity (16). However, because various other uterine tumors can also have similar signal intensity on MR imaging, further evaluation for the heterogeneous leiomyomas appears to be necessary. The purpose of our study was to analyze the patterns of heterogeneous leiomyomas and
to differentiate each type of secondary changes by means of MR imaging-pathologic correlation.

Received 3/6/97; Accepted 3/12/97

[3] To whom correspondence should be addressed, at Department of Radiology, Asan Medical Center, University of Ulsan, Seoul 138-040, Korea. Fax: (82) 2-476-4719

2. MATERIALS AND METHODS

Our study consisted of thirty-six cases of leiomyomas with heterogeneous signal intensity on MR images from the same number of patients. The patients' ages ranged from 21-59 yrs (mean, 38 yr). MR imaging was performed to evaluate hypermenorrhea or dysmenorrhea (n = 20), palpable abdominal mass (n = 16), abnormal uterine bleeding (n = 12), enlarged uterus (n = 8), or for other reasons (cervical carcinoma in 2; adnexal diseases in 4). Surgery was performed within 3 weeks of MR imaging; myomectomy was performed on 14 patients and hysterectomy in 22.

After reviewing the MR images of all patients, we attempted to classify the 36 heterogeneous leiomyomas into different patterns and then investigated the causative factors of each pattern by means of MR imaging-pathologic correlation. We also evaluated the relationship of the different patterns of heterogeneous leiomyomas to the patient age and tumor size. MR imaging analysis was made by the consensus of two investigators with knowledge of the diagnosis but without knowledge of the pathologic or surgical findings.

MR imaging was performed using a 1.5-T superconducting magnet (Signa Advantage; GE Medical Systems, Milwaukee). Spin-echo images were obtained in all patients with a 5-mm-thick section, 2.5-mm gap, a 24-cm FOV, and 2 excitations in all patients. T1-weighted images with a repetition time (TR) of 700 msec or less and an echo time (TE) of 30 msec or less (TR/TE = 700/30) were obtained. T2-weighted images with a TR of at least 1, 800 msec and a TE of 60 msec or longer were also acquired. All patients were imaged in the transverse plane with T1- and T2-weighted sequences, whereas only T2-weighted images were obtained in the sagittal plane. Additional axial and sagittal images enhanced with gadopentetate dimeglumine (0.1 mmol/kg or a maximum of 10 ml) were acquired in 23 patients; fat-suppressed T1-weighted images in the axial or sagittal plane were obtained in 15 of these patients.

The signal intensities of leiomyomas were assessed with respect to that of myometrium or endometrium. On T2-weighted images, hypointensity was a signal intensity less than that of the outer zone of the myometrium, if junctional zone was present, the intermediate signal intensity was the same as or greater than that of the outer zone of the myometrium but less than the endometrium, and hyperintensity was isointense to the endometrium. After administration of gadolinium-DTPA, a varying degree of contrast enhancement was noted in the tumor. Enhancement was mild when it was less than that of the myometrium and dense when it was greater than that of the myometrium.

The resected specimens were examined and sections of the cut surface of the tumors were prepared for microscopic examination. Blocks (10-15 mm^2) were taken from the tumors corresponding to the regions of interest on MR images, fixed in 10 % buffered neutral formalin, embedded in paraffin, and stained with hematoxylin and eosin.

3. RESULTS

All leiomyomas included in this study showed varying degrees and different types of pathologic degeneration; two or more degenerative changes were combined in 15 cases. Cellular leiomyomas were also confirmed in 6 cases. Tumor size ranged from 3 to 24 cm with a mean diameter of 9 cm. Tumor locations were intramural in 23 cases, subserosal in 8, and submucosal in 5. Of the 36 patients, leiomyoma in the uterus was single in 27 and multiple in 9.

The heterogeneous leiomyomas could be classified into 4 patterns depending on the morphologic appearance of signal intensities, i.e. speckled, nodular, cystic, or indeterminate (Fig. 1). The indeterminate pattern represented the cases in which signal-intensity morphology did not belong to the other 3 patterns. A speckled pattern was seen in 14 cases, nodular pattern in 11, cystic pattern in 9, and indeterminate pattern in 2. Specific relationship of the different patterns of heterogeneous leiomyomas to patient age and tumor size was not observed. The principal pathologic findings associated with each morphological pattern are summarized in Table 1. The speckled pattern (n =14) (Fig. 2) was associated with a mild degree of hyaline or myxoid degeneration or focal areas of necrosis. However, on conventional T1-and T2-weighted images, it was very difficult to distinguish each type of degeneration in a group having speckled pattern. The nodular pattern (n = 11) are mainly caused by necrosis (Fig. 3) or cellular leiomyoma. The cystic pattern (n = 9) (Fig. 4) indicated a disease with cystic change, commonly related to a severe hyaline or myxoid degeneration or necrosis. The indeterminate pattern (n = 2) was caused by either hyaline degeneration or focal necrosis.

The signal-intensity characteristics of each degeneration based on MR imaging-pathologic correlation are shown in Table 2. Of the 36 heterogeneous leiomyomas, hyalinization was a main secondary degeneration in 15 cases on pathologic examination and was mild in 10 and severe in 5. Precise MR imaging-pathologic correlation was achieved in only 5 cases in which severe hyalinization was diffuse. This correlation was very difficult in leiomyomas with a mild degree of hyalinization because of their interspersed involvement. The hyalinized areas were isointense on T1-weighted images, hypointense on T2-weighted images, and mildly (n = 4) or densely (n = 1) enhanced after administration of contrast material (Fig. 5).

Myxoid degeneration (Fig. 6) was present in 5 of the 35 cases. On T2-weighted images, these areas were hyperintense or intermediate in signal intensity on T2-weighted images with dense enhancement on contrast-enhanced MR images. Cystic degeneration was combined in 9 cases. These cysts contained a viscuos or bloodstained fluid. They appeared not only as mixed types of masses with cystic and solid components, but also mostly as cystic, unilocular or multilocular masses (Fig. 7). Of the 10 leiomyomas with necrosis, seven were hyperintense on T1-weighted images (diffuse form in 4 and ring-shaped in 3), and showed variable signal intensities on T2-weighted images; coagulative necrosis showed hypointensity on T2-weighted images. The 5 leiomyomas with necrosis in which contrast-enhanced images were obtained were not enhanced after infusion of the contrast material. A definite area of calcification was seen only 1 case and demonstrated a signal-void area on all pulse sequences. In 6 cellular leiomyomas (Fig. 8), signal intensity was hyperintense in 2 and intermediate in 4 on T2-

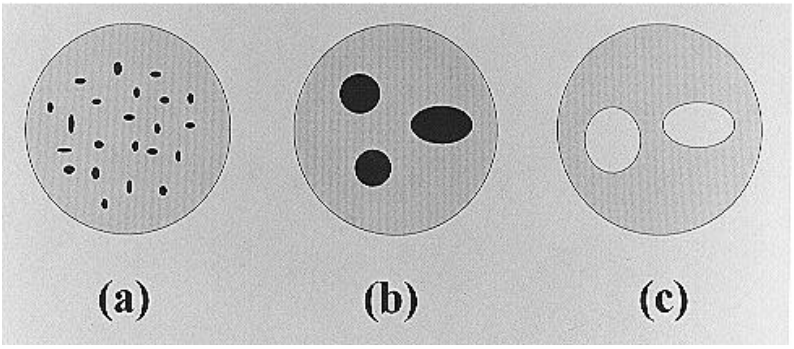

Figure 1. A schematic diagram showing patterns of heterogeneous leiomyomas according to the morphological appearances of signal intensity: (a) speckled; (b) nodular; and (c) cystic. The indeterminate pattern represents the cases in which signal-intensity morphology does not belong to (a), (b), or (c).

TABLE 1: The Relationship between Different Patterns of Heterogeneous Leiomyomas and Principal Pathologic Findings

	Speckled (n* = 14)	Nodular (n = 11)	Cystic (n = 9)	Indeterminate (n = 2)
Hyaline	10			1
Myxoid	3			
Necrosis	1	6		1
Cystic change**			9	
Cellular		5		

* n = number of cases.

**Cystic changes occurred in leiomyomas with severe hyaline (n = 4) or myxoid (n = 2) degenerations or necrosis (n = 2) or in cellular leiomyomas (n = 1).

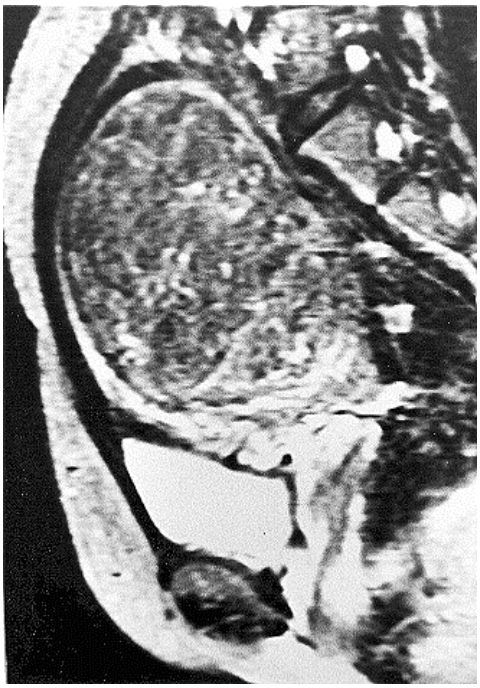

Figure 2. An intramural leiomyoma showing a mild hyalinization (speckled pattern) in a 21-year-old woman. A sagittal T2-weighted (2000/90) image shows a large mass with diffusely scattered, hyperintense spots in the uterus.

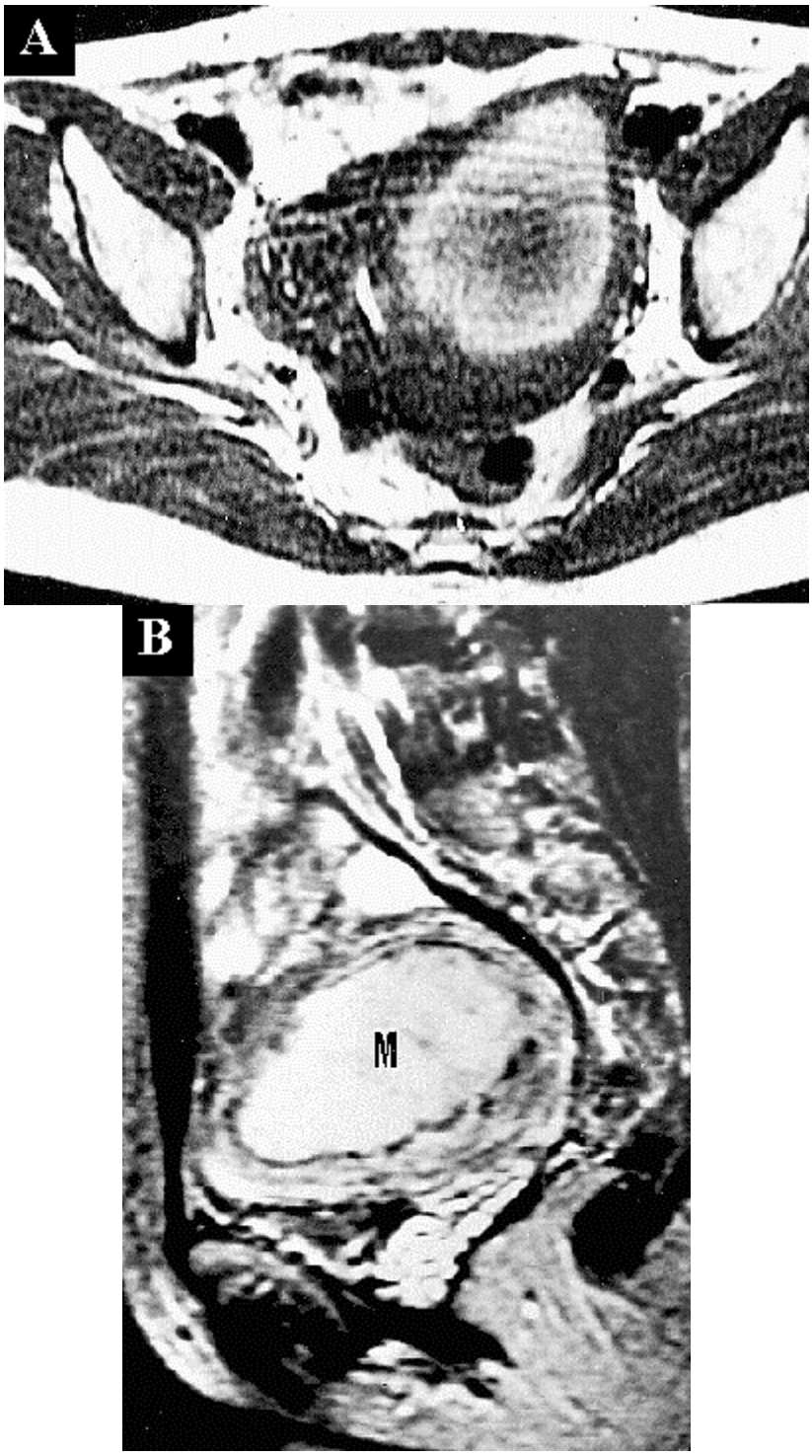

Figure 3. An intramural leiomyoma with necrosis and cystic change (cystic pattern) in a 37-year-old woman.
A, Axial T1-weighted (333/11) image shows a mass with hyperintensity in the uterus.
B, Sagittal T2-weighted (1800/80) image shows a hyperintense mass (M) with minimal heterogeneity in the uterus. A thin hypointense rim is seen to surround the mass and was confirmed to be the compressed myomatous tissue (pseudocapsule).

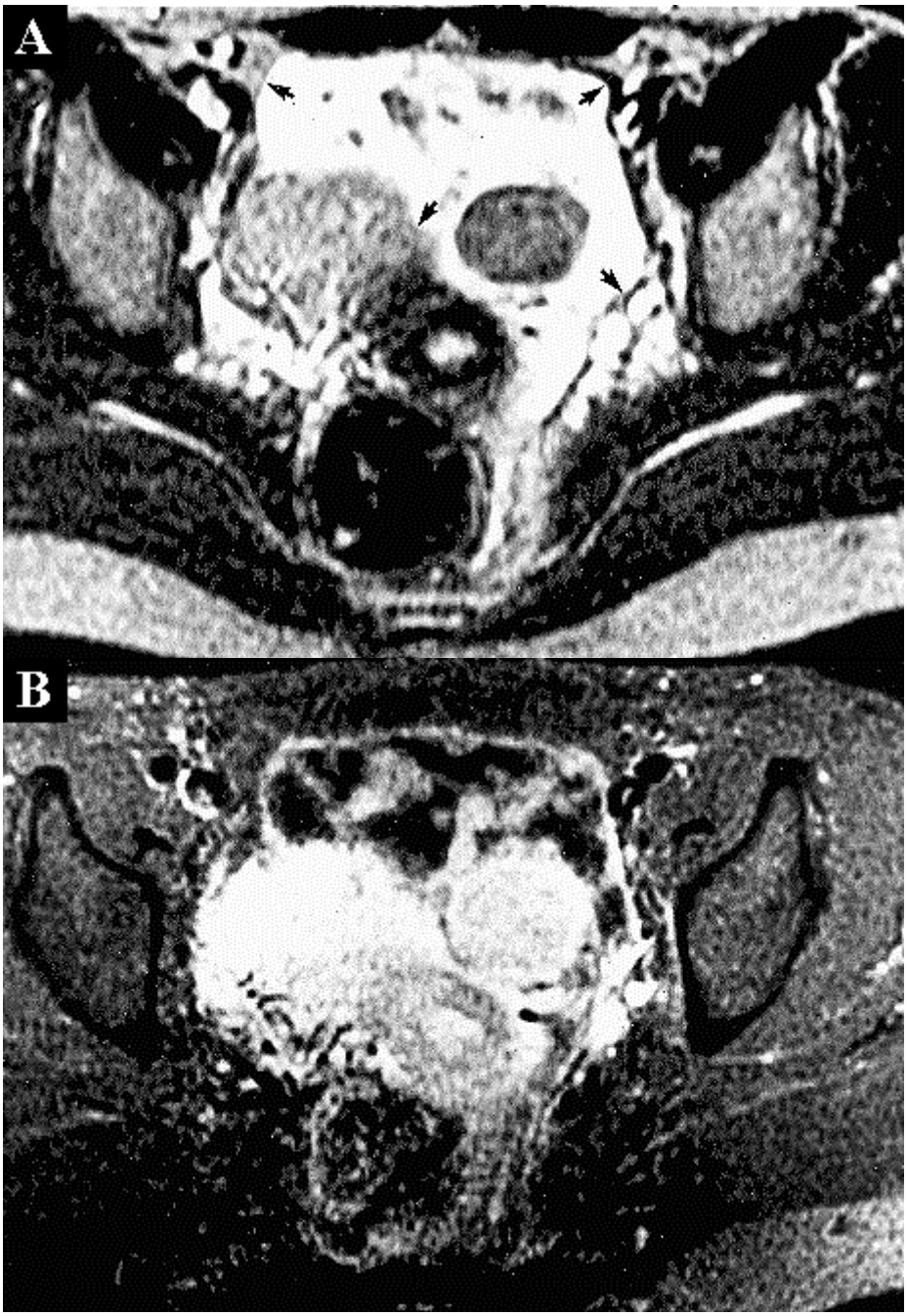

Figure 4. A subserosal leiomyoma with cystic degeneration (cystic pattern) in a 47-year-old woman, simulating an adnexal mass.
A, Axial T2-weighted (2000/80) image shows a mass (arrows) with hyperintense cystic area and islands of solid components.
B, Axial contrast-enhanced T1-weighted image with fat suppression (600/15) shows dense enhancement of the hyalinized myomatous tissues.

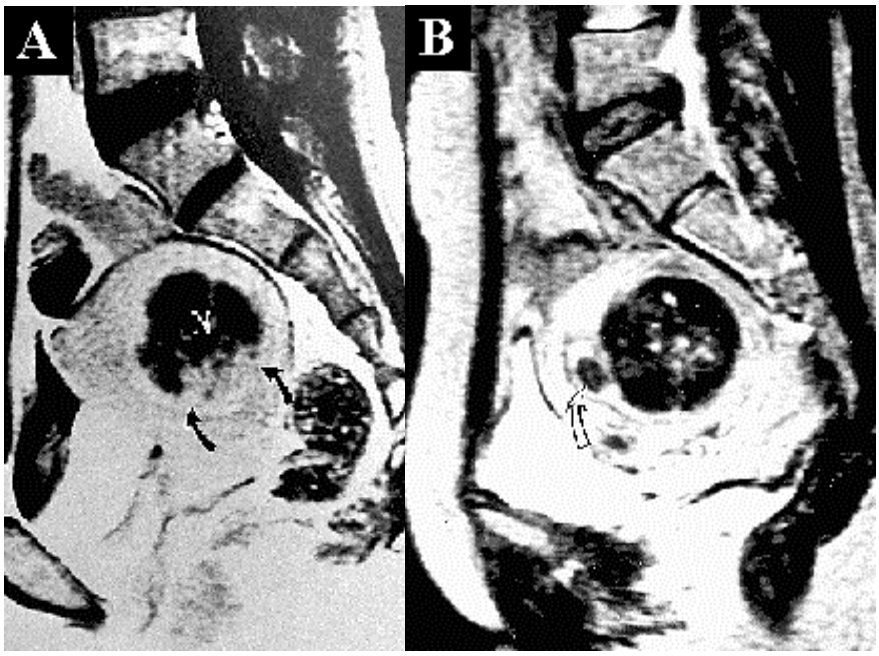

Figure 5. An intramural leiomyoma with coagulative necrosis and severe hyalinization (speckled pattern) in a 33-year-old woman.
A, Sagittal contrast-enhanced T1-weighted (566/11) image shows a mass with densely enhanced area (arrows) of severe hyalinization and nonenhanced area of coagulative necrosis (N).
B, Sagittal T2-weighted (2000/80) shows the same hypointensity in both areas of different pathologic changes. A small, nondegenerative submucosal leiomyoma (arrow) is also noted.

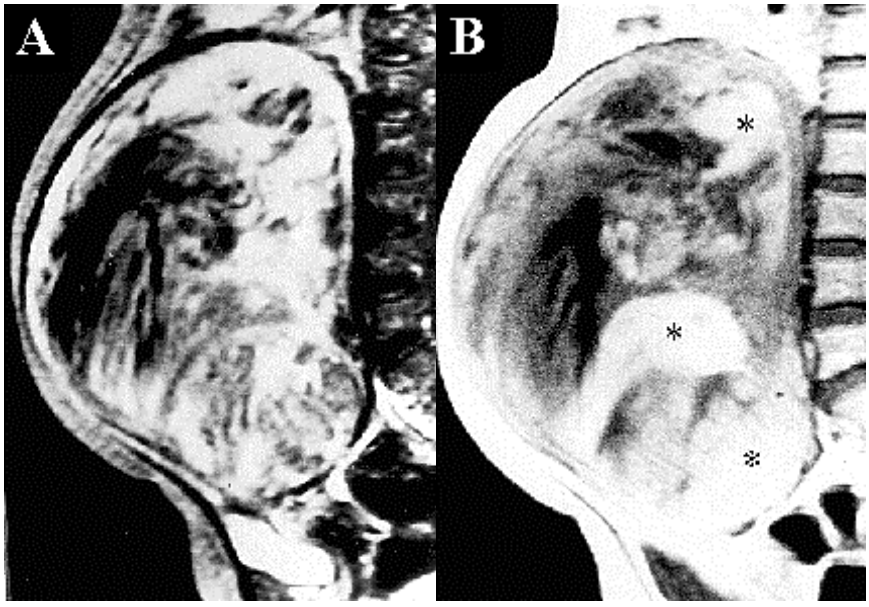

Figure 6. An intramural leiomyoma with myxoid and cystic degenerations and cystic changes (cystic pattern) in a 45-year-old woman.
A, Sagittal T2-weighted (2000/80) image shows a large heterogeneous mass in the uterus.
On pathologic examination, hypointense areas of the mass were caused by the area of hyaline degeneration, while the areas with intermediate signal intensity showed myxoid degeneration and hyperintense regions were due either to cystic changes or myxoid degeneration.
B, Sagittal contrast-enhanced (416/11) image shows dense enhancement of the areas with myxoid degeneration (*).

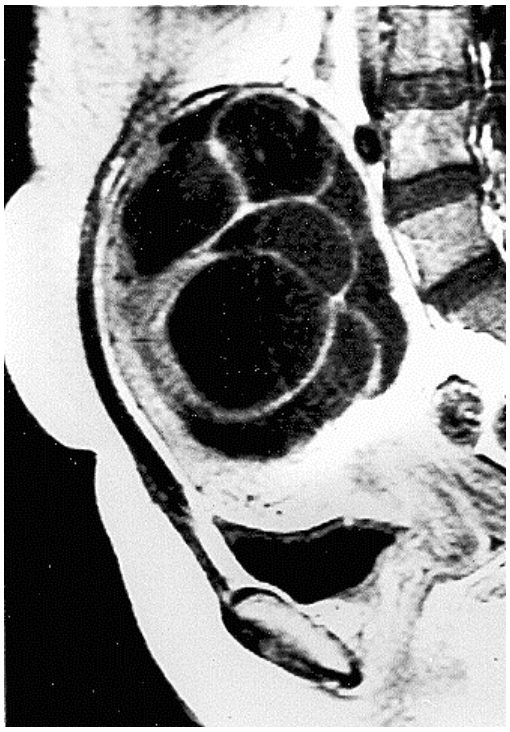

Figure 7. A cellular leiomyoma with multiseptate cystic appearance (cystic pattern) in 45-year-old woman.
Sagittal contrast-enhanced (566/11) image demonstrates a multiseptate cystic mass in the uterus. The cellular solid components are mildly enhanced.

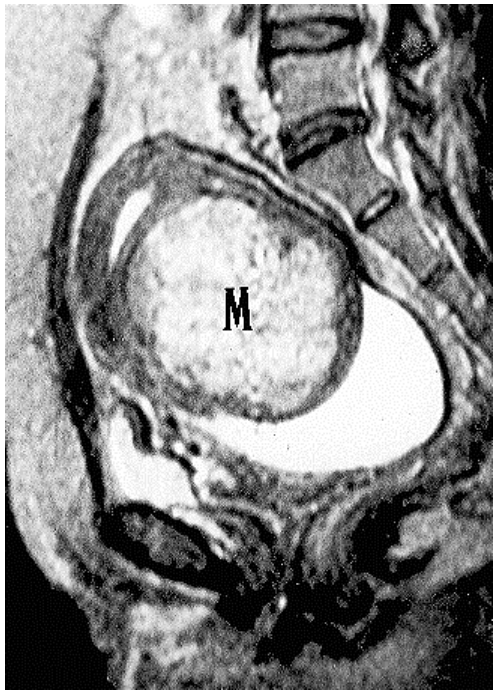

Figure 8. A cellular leiomyoma of intramural type (nodular pattern) in a 47-year-old woman.
Sagittal T2-weighted (2000/90) image shows a large, hyperintense mass (M) in the uterus. Fluid is collected in the cul-de-sac.

weighted images and showed homogeneity in 3 and heterogeneity in 3; the masses were mildly enhanced in 4 in which contrast-enhanced images were obtained.

In the periphery of the masses, a hypointense rim, less than 5 mm thick was noted on T2-weighted images in 13 cases (36%); the rim was mildly enhanced after infusion of contrast material. This type of rim was more commonly seen in the nodular (n = 7) or cystic (n = 5) than in the speckled (n = 1) pattern of leiomyoma, and corresponded pathologically to either compressed myometrium (n = 7), remaining nondegenerative myomatous tissues (n = 4), or hyaline degeneration (n = 2). A hyperintense rim was also visible on T2-weighted images in 8 cases and was densely enhanced on contrast-enhanced images, which was seen in either speckled (n = 5) or cystic (n = 3) patterns of leiomyoma and were pathologically consistent with a thin edematous zone. Both hypointense and hyperintense rims coexisted in 3 cases.

4. DISCUSSION

Although ultrasound is the first modality of choice for the evaluation of patients with a pelvis mass, MR imaging has proved to have a greater potential in depicting the size, number, and location of leiomyomas and the presence and extent of the degeneration (6). Also, MR imaging can be used to document the regression of leiomyomas after treatment with Gonadotropin-releasing hormone analogues (10, 16). Despite increasing knowledge about various pelvic diseases on MR imaging, the role of this modality in distinguishing different types of degeneration has been limited (1, 4, 14) because of overlapping findings on conventional T1-and T2-weighted images. Therefore, an additional use for contrast enhancement with gadolinium-DTPA was recently stressed by some researchers (10, 16).

The leiomyoma is one of the tumors which has varying types of degeneration, resulting in a broad spectrum of MR imaging findings. Our study showed that the speckled pattern of heterogeneous leiomyomas resulted from mild degree of various secondary degenerations such as hyaline or myxoid degeneration or focal necrosis. Although mild hyalinization was the most commonly seen in our series, primary causes of the heterogeneity in speckled pattern could not be determined on MR imaging. The nodular pattern was associated with necrosis or cellular leiomyoma. Since MR imaging findings were similar in either case on T2-weighted images, evaluation of T1-weighted images was important because the leiomyomas with necrosis commonly appeared to be hyperintense on T1-weighted images. If available, contrast-enhancement images were also helpful for their differentiation; the areas with necrosis were not enhanced while cellular leiomyomas were mildly enhanced. In addition, since nodular hyperintense (hemorrhagic) mass can result from other uterine diseases such as gestational trophoblastic tumor (7), intrauterine ectopic pregnancy (3), or uterine sarcoma (13), detailed clinical information is necessary to assess this nodular pattern of masses. The cystic pattern was commonly associated with severe hyaline or myxoid degeneration or necrosis. Subserosal leiomyomas with severe cystic change could be confused with adnexal masses, but the presence of a hypointense rim in the periphery of the mass on T2-weighted images aided in diagnosing leiomyomas.

Among various degenerative changes, hyalinization is the most common type of secondary degeneration, occurring in 63 % of uterine leiomyomas (11). The hyalinized areas within tumors microscopically consisted of eosinophilic bands infiltrating the muscle bundles with paucicellularity. Similar to those of nondegenerative myomatous tissues, hyalinized areas showed hypointensity on T2-weighted images, and after administration of gadolinium were, in most instances, mildly enhanced. Therefore, the cause of heterogeneity in hyalinized leiomyomas on T2-weighted images is unknown although possible relation to the other coexisting types of degeneration or cellularity of myomatous tissues surrounding the hyalinized areas can be speculated.

Myxoid degeneration in a leiomyoma, characterized microscopically by scattered nuclei embedded in an amorphous, fibrillar matrix, was present in 5 of our 36 cases. They appeared to be isointense on T1-weighted images and hyperintense on T2-weighted images. Interestingly, these areas were densely enhanced after the administration of the contrast material. Although the exact cause was not investigated in our study, we presumed that the dense enhancement was caused by increased vascular components in the fibrous tissue stroma surrounding the myxoid areas. Therefore, dense contrast enhancement in focal areas of the leiomyoma should not be used as a sign of sarcomatous degeneration.

Necrosis may result from torsion or twisting of a pedunculated leiomyoma and is often associated with pregnancy or the use of contraceptive drugs (8, 12). Unlike other types of degeneration, it produces clinical symptoms of abdominal pain and tenderness (2, 8). Such necrosis was characterized by diffuse or ring-shaped hyperintensity on T1-weighted images, hyperintensity or intermediate signal intensity on T2-weighted images, and nonenhancement after gadolinium administration. However, it should be noted that the presence of coagulative necrosis could be missed if contrast-enhanced MR images were not used since the signal intensity of coagulative necrosis

on T2-weighted was identical with that of the nondegenerative myomatous tissues.

Despite the low prevalences, the presence of calcification in a uterine mass is the most specific sign of a leiomyoma (15). Rather than extensive calcifications, focal microcalcifications are commonly seen (5). However, in these cases MR imaging can not play a role in their detection.

In conclusion, heterogeneous leiomyomas can be classified on MR imaging into different patterns by the morphological appearances of signal intensity within tumor, depending on the types and degrees of secondary changes, and MR imaging has a potential in distinguishing each type of secondary changes that occur in leiomyomas.

5. ACKNOWLEDGMENTS

We express our gratitude to Bonnie Hami, Department of Radiology, University Hospitals of Cleveland, Cleveland, OH, for her editorial assistance in the preparation of this manuscript.

6. REFERENCES

1. Lee J. K. T., Gersell D. J., Balfe D. M., Worthington J. L., Picus D. & Gapp :The uterus: in vitro MR-anatomic correlation of normal and abnormal specimens. *Radiology* 157 (1985), 175

2. Entmann S. S.: Uterine leiomyoma and adenomyosis. In: *Novak's textbook of gynecology*, p. 443. Edited by H. W. Jones III & A. C. Wentz. Williams & Wilkins, Baltimore 1988.

3. Ha H. K., Jung J. K., Kang S. J., Nam-Koong S. E., Kim S. J., Kim J. Y. & Shinn K. S.: MR imaging in the diagnosis of rare forms of ectopic pregnancy. *AJR* 160 (1993), 1229.

4. Hamlin J. D., Pettersson H., Fitzsimmons J. & Morgan L. S.: MR imaging of uterine leiomyomas and their complications. *J Comput Assist Tomogr* 9 (1985), 902.

5. Hendrickson M. R. & Kempson R. L.: *Surgical pathology of the uterine corpus*. Saunders, Philadelphia 1980.

6. Hricak H., Tscholakoff D., Heinrichs L., Fisher M. R., Dooms G., Reinhold & Jaffe R. B.: Uterine leiomyomas: correlation of MR, histopathologic findings, and symptoms. *Radiology* 158 (1986), 385.

7. Hricak H., Demas B. E., Braga C. A., Fisher M. R. & Winkler M. L.: Gestational trophoblastic neoplasm of the uterus: MR assessment. *Radiology* 161(1986), 11.

8. Merrill J. A., & Creasman W. T.: Disorders of the uterine corpus. In: *Danforth's obstetrics and gynecology*, p.1027. Edited by J. R. Scott, P. J. DiSaia, B. Hammond, & W. N. Spellacy: J.B. Lippincott Company, Philadelphia 1990.

9. Okizuka H., Sugimura K., Takemori M., Obayashi C., Kitao M. & Ishida : MR detection of degenerating uterine leiomyomas. *J Comput Assist Tomogr* 17 (1993), 760.

10. Persaud V., McPath D. C. P. & Arjoon P. D.: Uterine leiomyoma. Incidence of degenerative leiomyomas and a correlation of associated symptoms. *Obstet Gynecol* 35 (1970), 432.

11. Rosai J.: *Ackerman's surgical pathology*. C. V. Mosby, St. Louis 1989.

12. Shapeero L. G. & Hricak H.: Mixed mullerian sarcoma of the uterus: MR imaging findings. *AJR* 53 (1989), 317.

13. Togashi K., Ozasa H., Konishi I., Itoh H., Nishimura K., Fujisawa I., Noma, Sagoh T., Minami S., Yamashita K., Nakano Y. & Konishi J.: Enlarged uterus: differentiation between adenomyosis and leiomyoma with MR imaging. *Radiology* 171 (1989) 531.

14. Walsh J. W.: Comparison of ultrasound and computed tomography in the evaluation of pelvic masses. *Clin Diagn Ultrasound* 2 (1979), 229.

15. Yamashita Y., Torashima M., Takahashi M., Tanaka N., Katabuchi H., Miyazaki K, Ito M. & Okamura H.: Hyperintense uterine leiomyoma at T2-weighted MR imaging: differentiation with dynamic enhanced MR imaging and clinical implications. *Radiology* 189 (1993), 721.